https://doi.org/10.20965/jrm.2020.p0503

Paper:

Personalized Subjective Driving Risk: Analysis and Prediction

Naren Bao[*1], **Alexander Carballo**[*2,*3], **Chiyomi Miyajima**[*4], **Eijiro Takeuchi**[*1,*3], **and Kazuya Takeda**[*1,*2,*3]

[*1]Graduate School of Informatics, Nagoya University
Furo-cho, Chikusa-ku, Nagoya 464-8601, Japan
E-mail: bao.naren@g.sp.m.is.nagoya-u.ac.jp
[*2]Institutes of Innovation for Future Society, Nagoya University
Furo-cho, Chikusa-ku, Nagoya 464-8601, Japan
[*3]TierIV Inc., Open Innovation Center, Nagoya University
1-1-3 Meieki-cho, Nakamura-ku, Nagoya 450-6610, Japan
[*4]Department of Information Systems, School of Informatics, Daido University
10-3 Takiharu-cho, Minami-ku, Nagoya 457-8530, Japan
[Received January 17, 2020; accepted March 26, 2020]

Subjective risk assessment is an important technology for enhancing driving safety, because an individual adjusts his/her driving behavior according to his/her own subjective perception of risk. This study presents a novel framework for modeling personalized subjective driving risk during expressway lane changes. The objectives of this study are twofold: (i) to use ego vehicle driving signals and surrounding vehicle locations in a data-driven and explainable approach to identify the possible influential factors of subjective risk while driving and (ii) to predict the specific individual's subjective risk level just before a lane change. We propose the personalized subjective driving risk model, a combined framework that uses a random forest-based method optimized by genetic algorithms to analyze the influential risk factors, and uses a bidirectional long short term memory to predict subjective risk. The results demonstrate that our framework can extract individual differences of subjective risk factors, and that the identification of individualized risk factors leads to better modeling of personalized subjective driving risk.

Keywords: risk assessment, subjective risk, personalization, risk factor identification, lane change

1. Introduction

There is a Chinese saying, "Don't just know something, but also know why it happens," which means that if we want to be able to understand a phenomenon, we also need to know what causes it. Driving has become a common behavior in our daily lives, and because driving safety is critical, predicting the risk levels of the current driving state and detecting the cause of the risk are all important technologies, whether in ADAS or in autonomous driving systems. Therefore, in our study, we aim to predict driving risk for individuals. Yet, the definition of risk varies on studies and applications. In our study, *subjective risk* refers to a driver's ability to identify and respond to potential risk in traffic situations, while *objective risk* refers to the objective probability of being involved in an accident, which can be directly measurable from the environment, vehicle dynamics, and driving behaviors. The definition of driving risk in this study, and its related factors are illustrated in **Fig. 1**, in which, a comparison of the factors related to subjective and objective risk shows that subjective risk is influenced by driving task difficulty (such as a lane change in a crowded traffic), driving experiences, age, and even personality, most of which are not measurable. Research into the assessment of objective risk has a long history [1–5], however, the field of subjective risk assessment research, which seeks to understand human risk perception remains largely unexplored. Studies, i.e., [6,7] have noted an inverse relationship between the subjective risk of drivers and traffic accidents: if drivers are able to detect or predict risky driving situations, they have an opportunity to alter their driving behavior to reduce their risk of having an accident. If we can identify the key factors

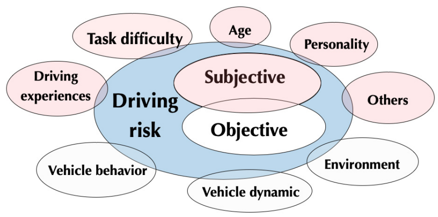

Fig. 1. Comparison of the factors that contribute to the perception of driving risk between subjective risk and objective risk.

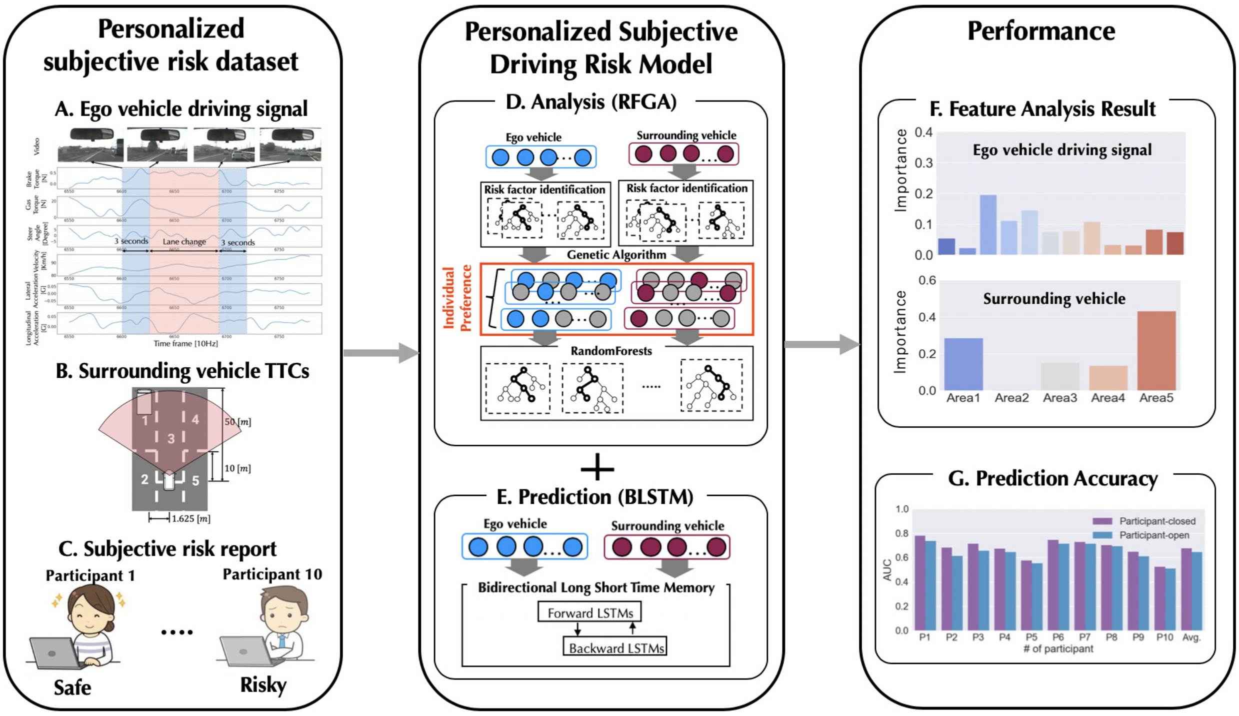

Fig. 2. Overview of our study including the dataset, personalized subjective driving risk model (PSDRM), and performance of analysis and prediction.

that drivers use to detect situational risk at key points in time, we may be able to reduce the probability of accidents [8, 9]. Therefore, we consider that causative factors and key timing are important for subjective risk modeling.

Along with the explosive development of modern artificial intelligence (AI) and sensor technology, there have been few studies to assess subjective risk. Most of them focused on risk assessment performance as in [10], a long short term memory (LSTM) was used to classify the driving scenes as risky or not. However, deep neural network-based methods have well-known limitations, including lack of interpretability of the key features and the reasons of model structure [11], thus, they could not explain why scenes were risky, or what driving-related information influenced these scenes to be risky. In addition, the reason why we feel risky is individual dependent, that is to say everyone has their own subjective risk assessment system. There are some studies conducted to model the individual subjective risk. In [12], the concept of RFind (risk feeling of individuals) was proposed, attuned to individual drivers, using a linear combination of 1/THW (time headway) and 1/TTC (time-to-collision). However, this risk index cannot be directly applied to adjust driving behavior.

To fill this gap, our work aims to: (i) explore which ego vehicle driving signals influence an individual's subjective risk and (ii) construct an effective method to predict the potential of subjective risk for specific users of ego vehicle driving signals and surrounding vehicle information. To achieve these two goals, we developed an integrated framework consisting of a risk factor identifier, based on random forests (RFs) methods optimized by genetic algorithms (GA), to identify important driving signal features related to personalized subjective risk. A subjective risk predictor based on a bidirectional long short term memory (BLSTM) model is used to predict the potential risk value of a lane change for several participants. Expressway lane change scenarios are selected, because changing lanes at high speed is relatively risky for drivers, and expressways do not have pedestrians or traffic signals so we were able to analyze participants' risk factors in straightforward manner. Our method was data-driven, i.e., it was based directly on the signals of the ego vehicle and surrounding vehicles, rather than on questionnaires. In **Fig. 2** the overall procedures and the kinds of dataset we used are illustrated. The proposed integration framework, the RFGA-BLTSM, efficiently combined an ensemble tree-based learning method with a sequential prediction deep neural networks-based method. Our contributions in this study are as follows.

1. A data-driven machine learning method models individual assessment of driving risk (subjective risk) for lane change maneuvers.
2. A method to extract influential driving related factors in an explainable way.
3. A method to predict the subjective risk level of lane change maneuvers for different participants.

This paper is structured as follows. In Section 2, we introduce studies related to risk assessment and risk factor identification. We then outline personalized subjective driving risk model (PSDRM) in the Section 3. The methodology of PSDRM is explained in Section 4. The experimental evaluation results are described in Section 5 and overall discussion in Section 6. Finally we conclude this work in Section 7.

2. Related Works

As stated before, we had two goals for this study. The first was to identify and investigate the factors which influence subjective risk for individuals, and the second was to construct an accurate model of the subjective risk assessment of each participant. Previous works related to these two goals are discussed in this section.

2.1. Risk Assessment

In recent years, thanks to the rapid development of sensor technology and hardware, the collection of driving data has become more accessible and affordable. At the same time, data-driven approaches have increasingly been used in risk assessment.

2.1.1. Objective Risk

Based on these developments, methods for machine learning have also been applied to the problem of objective risk estimation. Currently there are two main types of risk estimation algorithms: deterministic algorithms and probabilistic algorithms. Probabilistic algorithms estimate the degree of risk by calculating the probability distribution of a collision between a vehicle and surrounding objects. In [2, 4], collision risks were estimated as stochastic variables and were predicted for a short period of time into the future through the use of hidden Markov models and Gaussian processes. In [13], the risk of an accident was computed as a conditional risk using a graphical model, and this probabilistic risk was used for making go or no-go decisions. In another study [14], motion planning based on risk potential optimization was demonstrated. Probabilistic risk assessment can manage dynamic environments and uncertainty as stochastic variables, however the calculation cost of probabilistic approaches is extremely high. In contrast, deterministic risk estimation methods have the advantages of high computational efficiency and relatively ease of development. Various risk estimation measurement indices, such as TTC (time-to-collision) and THW (time headway), have been analyzed and compared for deterministic risk assessment [1, 15]. There is little doubt that objectively risky situations are hazardous, and earlier studies have focused on the avoidance of objective risk [5, 7, 16–18]. However, other studies [19] have rejected the idea that objective risk is a primary determinant of driving behavior, suggesting instead that drivers generally seek to avoid subjectively risky situations, and that behavioral adjustments are made to match these subjective risk estimates with a target level of acceptable risk [20]. Therefore, we preferred to focus on modeling subjective risk, which is more effective for capturing driving behavior.

2.1.2. Subjective Risk

Regarding to subjective risk assessment, investigation into the relationship between risk perception and accidents also has a relatively long history. The most challenging point of subjective risk assessment is the definition of subjective risk, which is not clear [21, 22]. Not to say that the influential factors of risk perception may contain such a variety of possibilities [6–8, 10, 23], such as the physical abilities of the drivers, the dynamic surrounding obstacles, driver workload, mental condition, the demographic information such as age, and gender. If we summarize all these factors as individual differences, most of the information could not be directly observed from driving data. This would lead to the result that real time risk analysis and estimation could not be conducted. However, one thing that is certain is that subjective risk perception influences driving behavior [24, 25]. Thanks to the rapid development of machine learning technology and a data-rich environment, some studies began to assess subjective risk using data-driven approaches. In [26], for example, an index of the driver's longitudinal perceptual risk estimate (PRE), along with TTC, THW and others features for detecting abnormal timing of braking, was proposed. Furthermore, in [12], the concept of RFind was proposed, which is an extension of the notion of risk feeling (RF) attuned to individual drivers, using a linear combination of 1/THW and 1/TTC. However, the reasons why certain factors influence subjective risk remain unclear. Therefore, different from other works, we aim to model subjective risk using data-driven approaches to identify individual subjective risk factors to unlock this black-box, using directly measurable driving signals, at the same time to predict subjective risk levels for individuals effectively.

2.2. Risk Factor Identification

Risk factor analysis and identification has long been a data-based field of research, with the use of risk evaluation questionnaires collected from study participants used for statistical analysis in [22, 27–31]. More recently, the use of behavioral and physiological data, as well as other data-driven approaches, has become more prevalent. In [32] negative binomial regression was used to identify factors for predicting an individual's driving risk, indicating that a driver's age and personality, and critical incident rate had an significant impact on crash and near-crash rates. Further research is needed into factors that trigger a driver's perception of risk, and on methods that could be used for personalizing the level of acceptable risk in autonomous driving systems, for example. Different from listed works, in our previous work [33], we compared driving signals that influenced the perception of individual drivers' subjective risk during lane changes. In this study, we expand our work by attempting to comprehensively identify the important factors that influence the perception of risk by drivers, by examining ego vehicle

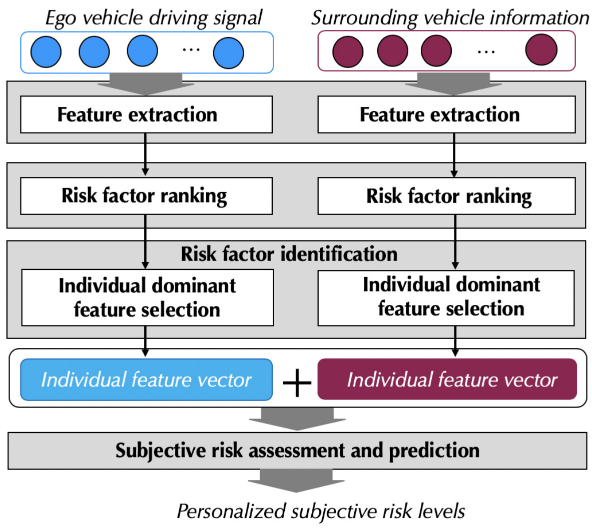

Fig. 3. The pipeline of the proposed PSDRM.

driving behavior signals, the location of surrounding vehicles, and lane change timing. We apply a GA to find the optimal RF structure. These personalized random forests structures with individual selected features should give us an insight, and explain how our personal driving behavior reflects our perception of subjective risk.

3. PSDRM

Our work focused on employing data-driven machine learning techniques to first investigate the factors that influence subjective risk (in machine learning terms: features) to interpret driving preferences on ego driving signals and surrounding vehicle signals, and to predict subjective driving risk levels.

To achieve these two goals, as illustrated in **Fig. 2**, our subjective risk dataset include (A) ego vehicle driving signals (in our study, we extracted braking force, acceleration force, steering angle, velocity, lateral acceleration, and longitudinal acceleration from a controller area network (CAN)), and (B) surrounding vehicle TTCs are extracted to quantify the driving behavior and environment. The subjective risk report of ten participants (C) after they viewed the same lane change in front-view camera videos were selected as the target personalized variables. The PSDRM consisted of (D) an analysis of the features that influence ego vehicle driving signals and surrounding vehicle locations using the RFGA, which combined RFs with GA optimization, and (E) a prediction of subjective risk using 3-seconds data right before lane change start using a BLSTM. In **Fig. 3** the pipeline of the proposed architecture is introduced, which comprises of four steps.

1. Feature extraction: first, the dynamic features of the ego vehicle driving signals and the TTC values of the surrounding vehicle information were extracted. The dynamic features were extracted to capture the changes of driving behavior over time.

2. Risk factor ranking: next, we applied an RF based method to rank features, in order to visualize and intuitively understand the individual differences in the influential factors of subjective risk. Our purpose for this study was not only to predict the risk levels of a lane change maneuver, but also to analyze the important ego vehicle-related signals that influence an individual's risk perception. To address this problem, we adopted RFs [34] to identify the important features of subjective risk assessment. The explainability of a data-driven model is important for human users to understand why it can predict, so that we can appropriately trust. More and more related works began to address this problem, e.g., the 2016 ICML Workshop on *Human Interpretability in Machine Learning* [35]. Recently a new DARPPA program on explainable AI [36] showed the importance of an explainable model, and mentioned that RFs are more interpretable for their ensemble tree-based structure compared with deep neural networks. Furthermore, RFs can calculate the influence of features on the classification results [37, 38], so in our work feature importance are ranked to show the individual differences in subjective risk factors.

3. Risk factor identification: in order to adaptively select the number of influential risk factors, we proposed RFGA which used GA to optimize the RFs parameters of the tree-structure, selected features, and optimal forest size. RFs are powerful because they randomly select features to reduce the effect of the variance on the classification result, thus we still consider GAs to capture the individual differences when building tree structure, so that we could obtain a framework with which to build an accurate subjective risk assessment model with personalized feature selection.

4. Subjective risk assessment and prediction: the last step was to concatenate the individual dominant features to predict subjective risk levels for specific target participants. The BLSTMs were applied as a sequential prediction method, because our target risk level was reported after subjects viewed videos of a sequence of lane change maneuvers.

To validate our risk factor identifier and predictor as shown in **Fig. 2**, the performance of our model is shown as (F) the feature analysis result for ego vehicle driving signals and surrounding vehicle locations for both right and left lane changes, and for different time segments using before, during, and after lane change data and, (G) the subjective risk prediction accuracy of participant-closed and participant-open experiment. Participant-closed was a prediction experiments that used the data of one participant in the training and test phases, while participant-open was a prediction experiment that used the data of different participants in the training and test phases.

4. Methodology

In this section, we introduce the details of our dataset, including how we set up ground truth for subjective risk, and the methodology for conducting risk factor identification and prediction with the PSDRM.

4.1. Dataset

A subset of the NUDrive dataset [39] was used as our data in this study. Several data were collected using an instrument-equipped test vehicle, which was driven on the road in Nagoya City, Japan. A subset of the data used in our study consisted of 859 video clips of lane changes captured using a forward-facing camera, as eleven different drivers executed lane changes on a Nagoya expressway. All the drivers followed the same route, and were asked to drive as they normally do, as much as possible, while conducting lane changes as often as possible. A video of the entire trip for each driver was then parsed manually to extract the lane change scenes. In this study, subjective risk perception feedback was collected from our participants as they viewed the lane change video clips described above, using the annotation procedure described in Section 4.1.1. The method used to extract that were likely to influence the perception of risk, which included ego vehicle driving signals and surrounding vehicle location information, is explained in Section 4.1.2.

4.1.1. Data Annotation

To properly model subjective risk perception with individual differences requires a large amount of related factors, such as age, driving experience, and task difficulty as shown in **Fig. 1**, and demands a very complex high-dimensional distribution. To reduce cost of collecting such data, Japanese drivers were selected through a random sample as experiment participants. We narrowed down our target participants as non-expert drivers of a similar age, and asked all the participants to watch the same lane change videos to reduce the influence of demographic variables so as to model their latent personality. Ten participants (five male and five female) with an average age of 44 years (SD = 5.2 years) were recruited randomly without knowing the purpose of this experiment in our subjective risk assessment experiment. All the participants had a valid driver's license and an average of more than 16 years of driving experience.

Prior to the experiment, the data collection procedure was approved by the ethic committee of the Institutes of Innovation for Future Society at Nagoya University on October 8th, 2015 (approval number KIEI-1), to guarantee the safety and privacy of the participants. The participants were asked to fill out a demographic survey, and were then asked to view video clips of lane changes on a video player installed in a notebook computer, while marking a score sheet with the level of risk they perceived during the lane changes. The videos were recorded using a forward-facing camera, and included images from 3 s before each lane change until 3 s after the lane change was completed. All the participants were asked to view the same 859 lane change video clips (432 lane changes to the right and 427 lane changes to the left) without any knowledge about who was driving the vehicle. Each of the lane change video clips varied in length, with an average length of 12.64 s (MD = 12.64 s, SD = 1.30 s). As they viewed each lane change, the participants were asked to report the level of risk perceived on a keypad, using a 5-point Likert-scale [40] for the risk level score, as follows: 1 = *very safe*, 2 = *safe*, 3 = *neither safe nor unsafe*, 4 = *risky*, 5 = *very risky*. The participants only observed driving videos on a computer, so they did not perceive any inertial force in response to car movement. Furthermore, information about surrounding vehicles that was not recorded by the front-view camera, could not be observed, thus the observed surrounding area is illustrated in **Fig. 4**. In order to prevent habituation by the experiment participants, the sequence of videos was randomly shuffled, so that participants would not observe videos from the same driving sequence.

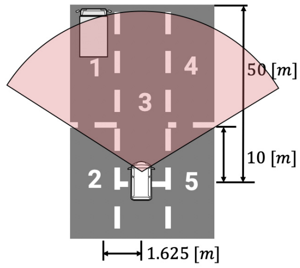

Fig. 4. Area codes used to represent the locations of surrounding vehicles. TTC values for the nearest vehicles in each of the five areas shown above were measured during each time interval.

4.1.2. Feature Extraction

The ego vehicle driving signals (braking force, acceleration force, steering angle, velocity, lateral acceleration, and longitudinal acceleration) were taken directly from the vehicle's CAN, while the TTC values for the surrounding vehicles were calculated using relative velocity and distance information from the radar sensor data. These two types of data were synchronized to 10 Hz. The relationship between the content of the lane change videos and the raw driving signal data from the ego vehicle is explained in **Fig. 5**. The dynamic features of the ego vehicle driving signals and the surrounding vehicle location data also offer a wealth of information about subjective risk perception, because lane change behavior varies over time in response to the presence of surrounding vehicles and to differences in the driving environment. Our method of designating the locations of surrounding vehicles is shown in **Fig. 4**. Because participants could only observe surrounding vehicles that were visible in the video captured by the forward-facing camera, the effect of vehicles located behind the ego vehicle was not analyzed

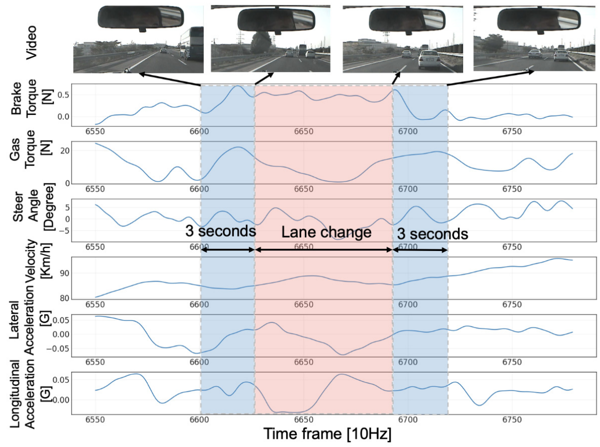

Fig. 5. Relationship between the content of the lane change video clips and raw signal data from the ego vehicle. During our collection of subjective risk ranking data, all participants were asked to view the same lane change videos, without knowledge of who was driving the vehicle.

Table 1. Features likely to influence subjective risk.

Categories	#	*Description*	*Features*
	1	Braking force	b
	2	1st order brake force	$\dot{b}$
	3	2nd order brake force	$\ddot{b}$
	4	Accel force	a
Ego	5	1st order accel force	$\dot{a}$
vehicle	6	2nd order of accel force	$\ddot{a}$
driving	7	Steering angle	θ
signals	8	1st order steering angle	$\dot{\theta}$
	9	2nd order steering angle	$\ddot{\theta}$
	10	Velocity	v
	11	Lateral acceleration	ω
	12	Longitudinal acceleration	L
	13	TTC of the nearest vehicle in area #1	TTC_1
Surrounding	14	TTC of the nearest vehicle in area #2	TTC_2
vehicle	15	TTC of the nearest vehicle in area #3	TTC_3
location	16	TTC of the nearest vehicle in area #4	TTC_4
	17	TTC of the nearest vehicle in area #5	TTC_5

in this study. TTC values for the nearest vehicle in each of the surrounding areas were also calculated when the surrounding vehicle information was captured. We defined our dynamic features using the same linear regression coefficients as those proposed in [41], as shown in Eq. (1).

$$\dot{o}(t) = \frac{\sum_{n=-N}^{N} n \cdot o(t+n)}{\sum_{n=-N}^{N} n^2} \quad \dots\dots\dots\dots \quad (1)$$

where $o(t)$ is a static feature of raw driving signals at time t. Examples of these static features include b (braking force), a (acceleration force), and θ (steering angle). N represents the size of the half-window used to calculate the coefficients. We determined the regression window to be $2N = 1000$ ms for both first and second order features of the raw signals through experimental evaluation.

The features extracted for our study are summarized in **Table 1**, and consist of 17 features in total, divided into two categories, which are ego vehicle driving signals and the surrounding vehicle locations. The first order dynamics of these features were calculated using Eq. (1), and the second order dynamics of these features were calculated by using Eq. (1) a second time, based on the first order dynamics.

4.1.3. Personalized Subjective Risk

In order to visualize individual differences in subjective risk while watching the same driving videos, t-distributed stochastic neighbor embedding (t-SNE) [42] was applied to reduce the feature space of 12 dimensional ego vehicle driving signals into two dimensions so that one lane change maneuver could be marked as one scatter point. We visualize all lane change maneuvers on a map illustrated in **Fig. 6**, in which five risk levels are marked by different marker shapes for ten participants. From this visualization, we observe that individual participants reported different risk levels (different marker configurations) for the same lane change maneuvers (the same point in the figure).

4.2. Lane Change Scenario

Lane changes were selected as the driving risk assessment scenario for our study, because lane changes on expressways are considered to be relatively risky [43]. In this study, lane changes were divided into two types (lane changes to the right and to the left), and into three chronological segments (before, during and after the lane change) as shown in **Fig. 7**. We did this in order to investigate individual differences in risk perception related to the type of lane change, as well as differences that might occur during various chronological segments of the lane changes.

4.3. Risk Factor Identification Using RFGA

To formalize this problem, we considered our dataset as X, and each lane change was defined as X_n, the n-th lane change data included a set of k features, and Y was the class labels set such that $y_n \in \{1, \dots, 5\}$ as shown in Eq. (2), where 1 = very safe, 2 = safe, 3 = neither safe nor unsafe, 4 = risky, 5 = very risky. There were three parameters of the RFs to be determined, which were *ntrees*: the number of trees, *mtry*: the node size for stopping the split, and k: the optimal number of features selected to represent the individuals. The accuracy was the averaged classification area under the curve (AUC) score.

$$X_n = \begin{bmatrix} x_{11} & x_{12} & \cdots & x_{1k} \\ \vdots & x_{22} & \cdots & \vdots \\ \vdots & & \ddots & \\ x_{t1} & \dots & & x_{tk} \end{bmatrix}_n, \quad Y_n = [y] \quad . \quad . \quad (2)$$

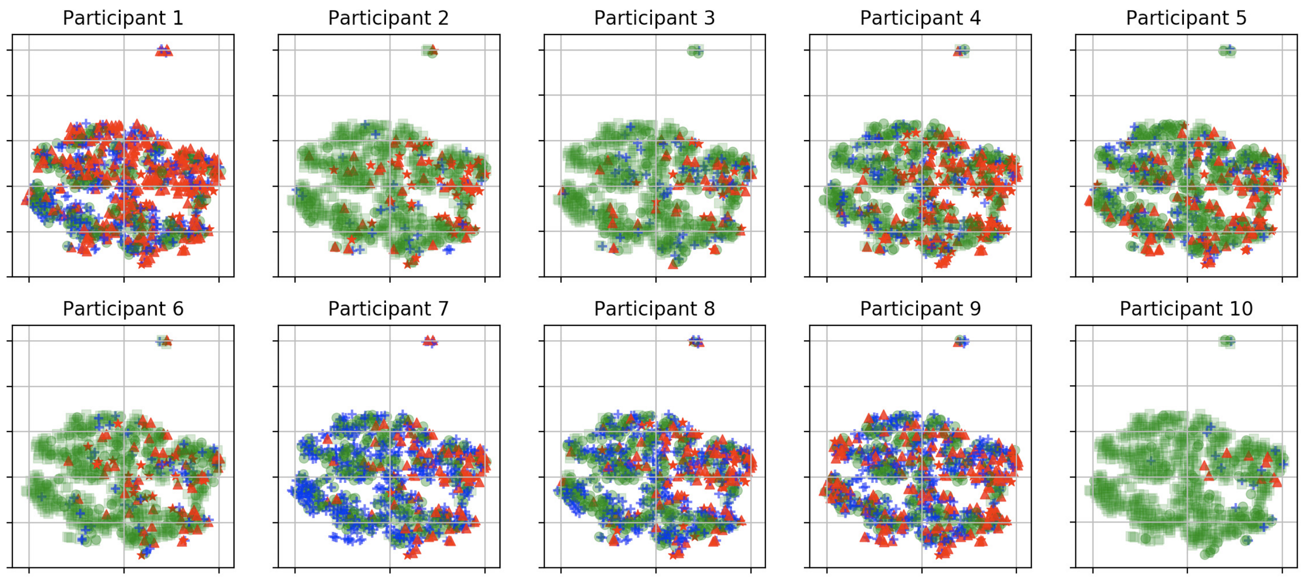

Fig. 6. Individual differences in reported subjective risk levels by ten participants for all lane change maneuvers. The dimensions reduced by t-SNE are represented on the X-Y axes. The t-SNE results show little correspondence between participants. Note that each data point in the participant's map represents the same lane change, however, because of individual differences, the plot shows different marker configurations. The markers used in this figure are ■: very safe; ●: safe; +: neither safe nor risky; ▲: risky; ⋆: very risky.

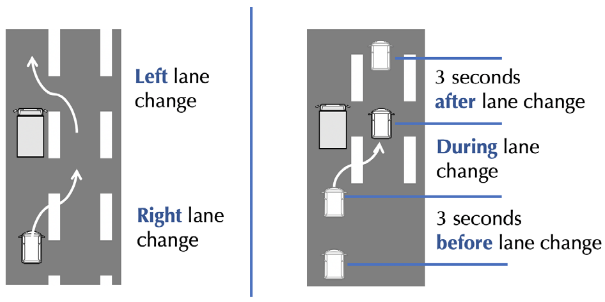

Fig. 7. Expressway lane changes were selected for modeling subjective risk during driving. Lane change data were divided into two categories, type of lane change (left) and chronological segment of the lane change (right).

where the sampled bootstrap dataset X_n, has a set of driving data and a set of risk levels Y_n with t time frames, and a feature vector V that represented the set of parameters to be optimized in order to maximize the accuracy of the RFs is shown in Eq. (3).

$$V = \begin{bmatrix} X_n^{k1} & X_n^{k2} & \cdots & X_n^{kK} & mtry & ntrees \end{bmatrix} \quad (3)$$

To find the optimal set of features for the RFs in the reduced feature space in the k dimension, where $1 \leq k \leq K$, $k \in \mathbb{N}$, K represents the maximum value of the feature space, which for the ego vehicle driving signals is 12, and for the surrounding vehicle directions is 5. We applied GA in a way similar to the approach in [44, 45] to select the dominant features for the different participants. We summarized our RFGA algorithm as **Algorithm 1**. **Algorithm 2** shows how we designed our fitness function to optimize the parameters of RFs, and **Algorithm 1** shows how the GA optimizes the parameter sets to find the best parameters for constructing the RFs.

Algorithm 1: Get optimal RFs using GA.

RFGA(Dataset)
begin
- $v, c, m \longleftarrow$ hyper-parameters
- $V \longleftarrow prepareV(Dataset)$
- $g \longleftarrow 0$
- $G_g \longleftarrow$ generate random v solutions from V
- $fitness \longleftarrow computeFitness(s) \forall s \in G_g$
- **while** $fitness \leq T_f$ and $g \leq N_G$ **do**
  - $G_g \longleftarrow crossOverAndMutate(G_g, c, m)$
  - $fitness \longleftarrow computeFitness(s)\ \forall s \in G_g$
  - $g \longleftarrow g+1$
- **return** (fittest solution)

Algorithm 2: Compute fitness for random forests.

computeFitness(solution)
Result: Accuracy of the Random Forests
begin
- $A \longleftarrow solution$
- $Chromosome \longleftarrow getChromosome(A)$
- $k, ntrees, mtry \longleftarrow decode(Chromosome)$
- $A_g \longleftarrow decomposeSet(A, k, ntrees, mtry)$
- $model \longleftarrow fitRF(A_g, ntrees, mtry)$
- $accuracy \longleftarrow evaluate(model)$
- **return** $(accuracy)$

Algorithm 2 decodes the chromosome from the solution using ($getChromosome(..)$) inside ($decode(..)$) to extract the set of k values along with the $ntrees$ and

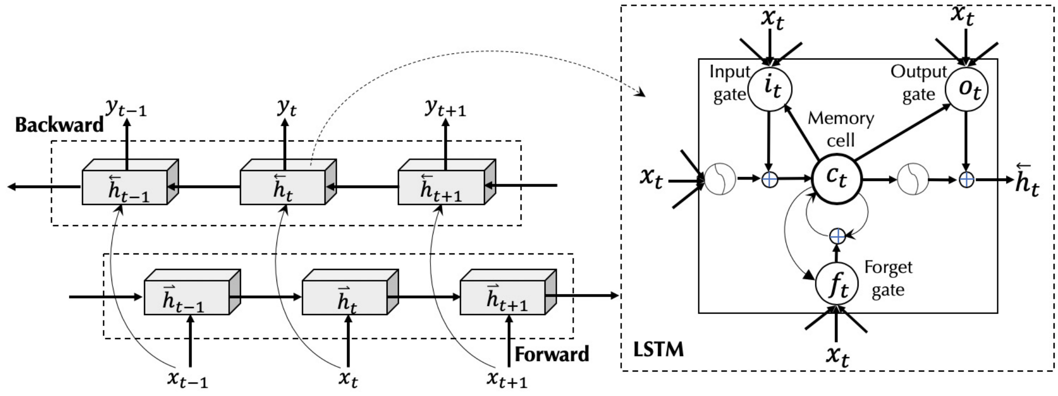

Fig. 8. Unfolded BLSTM network with LSTM units.

mtry values in the g-th generation. Following the decoding and as outlined in **Algorithm 2** the decomposition (*decomposeSet*(..)) is applied to the subset according to the solution's gene (the parameter sets), and then an RF model is fit by (*fitRF*(..)) on the decomposed solution A_g with the number of features used at each split (*ntrees* and *mtry*). With the obtained *model* of the decoded parameter setting (gene), we calculate *accuracy* from (*evaluate*(..)), and return it as the *fitness* of the RFs.

Algorithm 1 begins with hyper-parameter setting, where v, c, m represent population size in one generation, and the crossover and mutation parameters respectively. The initial feature vector V is obtained by *prepareV*(..) in Eq.(3). Then the initial generation is $v : v < K+2$ parameters randomly generated from V, and we calculate the accuracy obtained by *computeFitness* in **Algorithm 2**. Until the fitness threshold T_f and the maximum generation amount N_G are satisfied, the algorithm will generate the solutions (individuals) G_g on parameter setting c, m. For each new individual, *fitness* will be calculated again by *computeFitness* to check whether this generation is the fittest. After the iteration, the algorithm return the *fittest solution* including the optimal parameters $k, ntrees, mtry$. In our study, we interpret these parameters to be personalized parameters for constructing RFs.

4.4. Subjective Risk Level Prediction

4.4.1. Full Model

To construct an effective predictor, we propose an approach that uses BLSTM [46] with all the related information from the ego vehicle driving signals and surrounding vehicle TTCs in a sequential model. The BLSTM includes two independent LSTM networks in a BLSTM module, while the LSTM is a special recurrent neural network model. Through a special gate structure, it can store and retrieve information over a long time. In **Fig. 8**, a BLSTM recurrent diagram with LSTM units is shown. The LSTM comprises three gate structures (input i, forget f, and output o), a memory unit controller cell c, two input and output activation units, and three peepholes connections. The input and output gates are used to control the block input and output of the cell, and the forgetting gates are used to control the memory and forgetting state of the cell. The peephole is connected to the status information before the gates that allows the cell to record more sequential information. Finally, the block output information is recurrent, and it connects to the block input and all other gates, which enables LSTM to model complex and long-term dynamic features, and solves the gradient disappearance problem caused by long sequences in traditional recurrent neural networks [47]. The forward mechanism of the LSTM can be expressed using the following equation [48].

$$\begin{cases} I_n = \eta\left(W_I x_t + R_I O_{t-1} + b_I\right) \\ i_t = \sigma\left(W_i x_t + R_i O_{t-1} + p_i \odot c_{t-1} + b_i\right) \\ f_t = \sigma\left(W_f x_t + R_f O_{t-1} + p_f \odot c_{t-1} + b_f\right) \\ c_t = i_t \odot I_t + f_t \odot c_{t-1} \\ o_t = \sigma\left(W_o x_t + R_o y_{t-1} + p_o \odot c_t + b_o\right) \\ O_t = o_t \odot \eta\left(c_t\right) \end{cases} . \quad (4)$$

where I, i, f, c, o, and O represent the block input, input gate, forget gate, memory cells, output gate, and block output respectively. t is the number of sequential data; x is the input feature of the nth sequence; W is the weight matrix; R is the recurrent weight matrix; b is the bias vector; p is the peephole weight vector; and the subscripts I, i, f, o respectively represent the block input, input gate, forget gate, and output gate. σ is the logistic sigmoid activation function. η is the hyperbolic tangent activation function, and $\odot$ denotes the point-wise product with the gate value.

Compared with the LSTM, the BLSTM solves the problem that LSTM can only get past information but not future information. As shown in **Fig. 8**, there are two independent LSTM networks in a BLSTM module. These two LSTM networks have different directions, one is a forward LSTM, and the other is a backward LSTM. The forward LSTM is mainly used to extract future information about the sequence data, while the backward LSTM is mainly used to extract past information about the sequence data. Finally, their results are connected to the

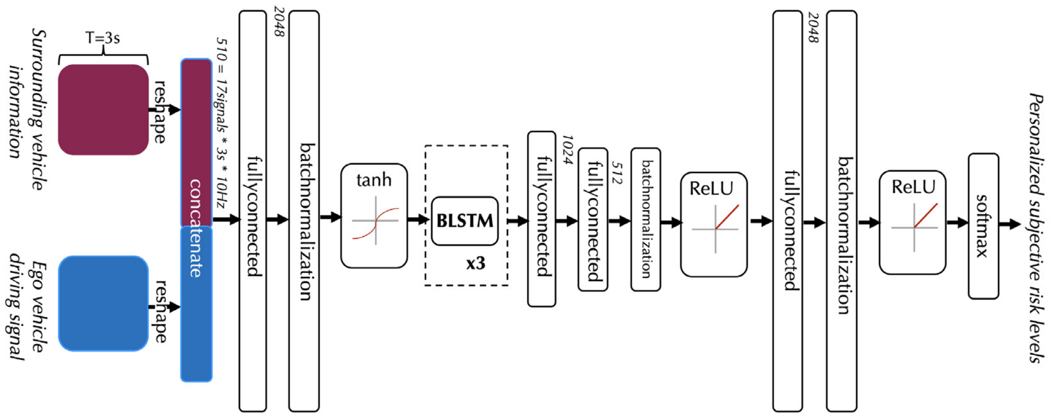

Fig. 9. Full model for personalized subjective risk prediction using BLSTM. All ego vehicle driving signals and surrounding vehicle location features are used for subjective risk prediction.

same output unit, and future and past features are fused to produce the output. In this way, the BLSTM is able to extract and fuse future and past features of the sequence data, which can be expressed using the following formulas [49].

$$\begin{cases} \overrightarrow{h}_t = \Gamma\left(W_{\overrightarrow{I}} x_t + W_{\overrightarrow{h}} O_{t-1} + b_{\overrightarrow{h}}\right) \\ \overleftarrow{h}_t = \Gamma\left(W_{\overleftarrow{I}} x_t + W_{\overleftarrow{h}} O_{t+1} + b_{\overleftarrow{h}}\right) \\ y_t = W_{\overrightarrow{y}} \overrightarrow{h}_t + W_{\overleftarrow{y}} \overleftarrow{h}_t + b_y \end{cases} \quad . \quad . \quad . \quad . \quad (5)$$

where $\overrightarrow{h}_t$ is the forward hidden sequence, $\overleftarrow{h}_t$ is the backward hidden sequence, and Γ is implemented by Eq. (4). y is the prediction of subjective risk for participants. We used averaged AUC score which represents the area under the receiver operating characteristic curve (ROC) as our evaluation criterion.

The architecture of the prediction model that used all the ego vehicle driving signals and surrounding vehicle location features is shown in **Fig. 9**. The core of the predictor is a three-layer BLSTM. Due to its recurrent nature, the model can be trained and evaluated on an arbitrary length of driving data. Because the participants viewed a driving video that included the 3 s before the lane change begun, we also extracted 3-seconds data before the lane change, including the ego vehicle driving signals and surrounding vehicle location, to predict the subjective risk.

4.4.2. Individual Model

To capture the individual differences in the influencing factors for subjective risk levels, we also built individual models that used RFGA to optimize RFs, and used the RFs a second time to predict subjective risk levels for participants. This model is shown in **Fig. 10**. The personalized RFs construction parameters $k_{ego}, k_{surr}, ntrees, mtry$ were selected by RFGA for each participant in **Algorithm 1**. The features selected by the personalized parameters are used to predict subjective risk using RFs for that participant. Because our individual model captures

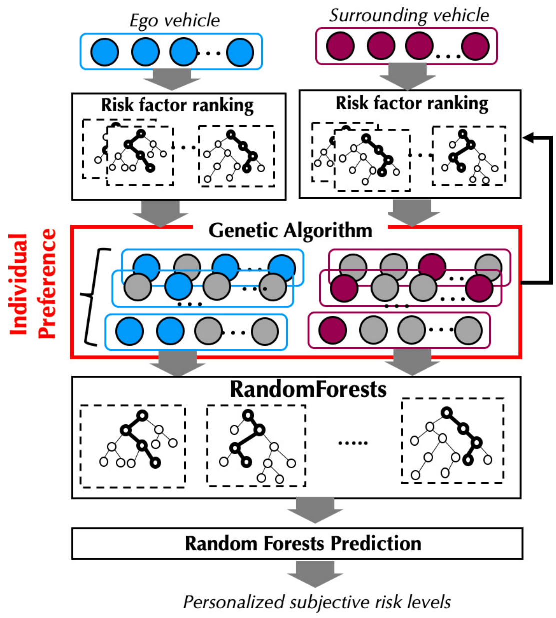

Fig. 10. Individual model for personalized subjective risk prediction using RFGA. Personalized parameters selected by RFGA are used for subjective risk prediction using RFs for each participant.

personalized feature selection, we consider it to be valid for personalized subjective risk prediction.

4.4.3. Integrated Individual Model

RFGA shows the explainability of RFs parameters for the tree structure, and the features selected by the GA. However, the RFs have a limitation on handling time series sequential data. Predictions that use the BLSTM with forward and backward layers can get not only past information but also future information. The subjective risk levels for participants were reported after they viewed the lane change maneuver videos, which happened along a time sequence. We proposed our PSDRM to integrate

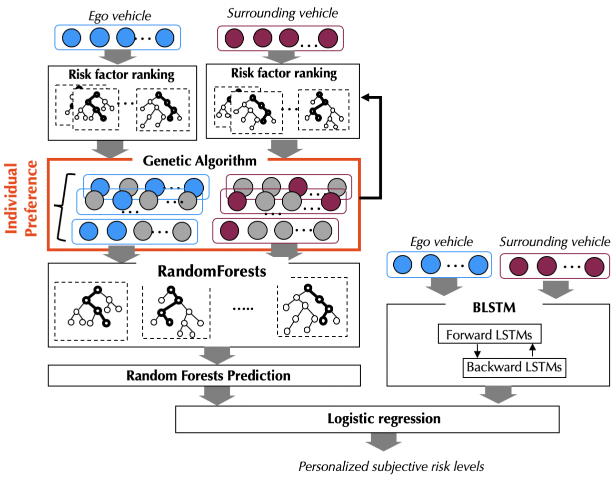

Fig. 11. Integrated individual model for personalized subjective risk prediction integrates RFGA with BLSTM to keep explainability by extracting personalized parameters and to predict subjective risk levels.

RFGA with BLSTM to maintain explainability by extracting personalized parameters and to predict subjective risk levels using all the input data. Logistic regression was used to combine these two models. The parameters for logistic regression were decided by experimental iteration. Logistic regression was used as a gate function to decide the weight of the individual and full models. The integrated individual model is illustrated in **Fig. 11**.

5. Experimental Validation

In this section, we evaluate our model in three steps. Firstly, we conduct an experiment for risk factor identification, and in this part, we investigate personalized parameters selected by RFGA, individual differences in the signals of the ego vehicle and the surrounding vehicle locations, with different lane changes time segments using RFs alone. Secondly, after determining the best combination of input signals, we conducted participant-closed and participant-open subjective risk forecasting before a lane change to compare with traditional methods. In our study, we define participant-closed experiments and participant-open experiments as follows.

1. Participant-closed experiment: the same participant data (were used) for training and testing.
2. Participant-open experiment: all participant data were mixed together for training, while model was tested on individual participant data.

Risk factor identification and prediction were mainly conducted in participant-closed experiments to validate whether dominant features for individual risk could be used to improve prediction accuracy, while participant-open experiments were conducted for comparison with general models. Lastly, we conducted subjective risk prediction during lane changes to compare between proposed models. 75% of the lane change data was used for training while the remaining 25% was used for testing the models. This allowed us to train our model with data from 644 lane changes, while 215 lane changes were omitted to be used later as test data, i.e., the test data were completely independent of the training set.

Table 2. Personalized parameters selected by RFGA.

	P1	P2	P3	P4	P5	P6	P7	P8	P9	P10
k_{ego}	2	1	4	5	5	4	4	6	6	5
k_{surr}	2	1	2	1	3	2	3	1	2	4
ntrees	100	30	100	30	50	100	50	100	50	30
mtry	7	3	5	5	7	3	7	3	5	3

5.1. Risk Factor Identification Result

k_{ego}, k_{surr} represent the optimal number of selected features for ego vehicle driving signals and surrounding vehicle location respectively, $k_{ego} \leq 12$, $k_{surr} \leq 7$, $k_{ego}, k_{surr} \in \mathbb{N}$, $ntrees \in \{10, 30, 50, 100, 300\}$ represents the number of trees and $mtry \in \{1, 3, 5, 7, 10\}$ represents the pruning node size used for constructing the RFs. The hyper parameters in **Algorithm 1** including the population size of one generation, and the crossover and mutation parameters, v, c, m were set to 50, 0.5, and 0.5 empirically. In addition, the fitness threshold T_f and the maximum number of generations N_G were selected to be the averaged AUC: 0.7 and 100 respectively. The parameters for personalized RFs selected by the GA are shown in **Table 2**. This result shows that by using RFGA, we can generate personalized RFs structure with an explicit parameter setting, and these parameters can be used to develop the PSDRM.

5.1.1. Ego Driving Vehicle Signal Ranking

To obtain an intuitive understanding of the influence of various driving signals on the risk assessment of individuals, we compared the driving signal ranking results when our participants were viewing lane changes to the left and right, which are shown in **Figs. 12** and **13** respectively. The y-axis represents feature importance for the ego vehicle driving signals. During the scenes of lane changes to the left, for all of our participants except P7 and P8, the most important feature for assessing subjective risk was velocity v, while the importance of the other features differed between the participants. These results show that when using an RF method, features other than velocity capture more individual differences in risk assessment. During the scenes of lane changes to the right, our feature analysis results revealed more individual variation in the importance of the various features. Velocity was still the most important feature for all of the participants except P7, P8, and P10, while a second tier of important features now included 2nd order dynamic brake $\ddot{b}$ and lateral acceleration ω for most of the participants.

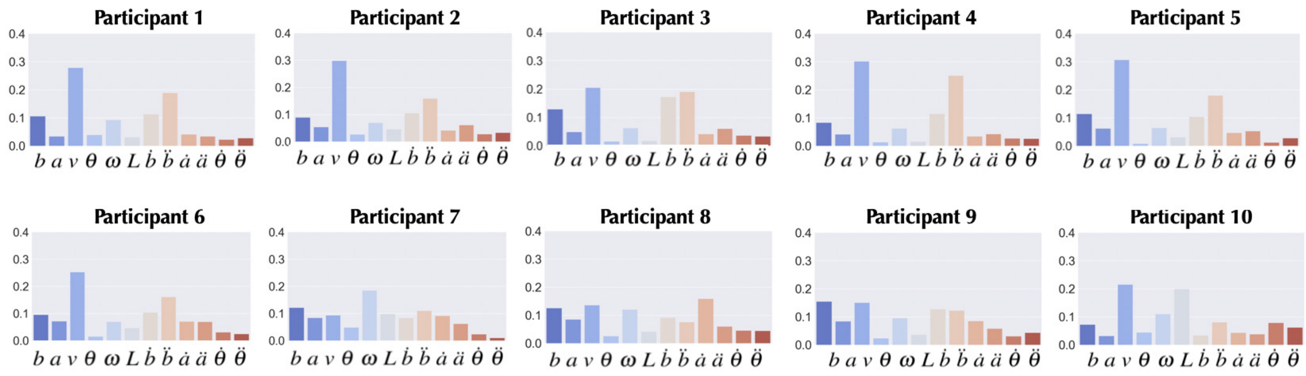

Fig. 12. Results of ego vehicle driving signal feature importance analysis during lane changes to the left. This result confirmed the variation in the perception of risk between individuals.

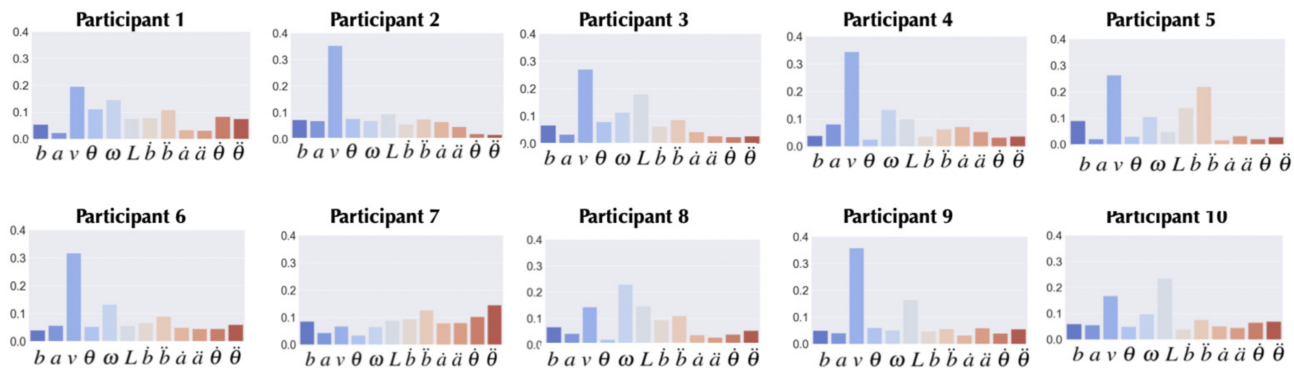

Fig. 13. Results of ego vehicle driving signal feature importance analysis during lane changes to the right. In Japan, the right lane of expressways is for higher speed driving and passing. Our feature analysis results for lane changes to the right showed more individual variation in the importance of the various risk factors.

In order to confirm the existence of individual differences in the relationship between driving signals and subjective risk, repeated one-way ANOVA tests were used to test the significance of the effect of differences in velocity on subjective risk between individuals. Participants 1 and 2 were selected for comparison because in both of their ranking results, velocity was the most influential feature during left lane changes, as shown in **Fig. 12** and during right lane changes in **Fig. 13**. A comparison of the test scores is shown in Appendix A (**Table 4** for participant 1, and **Table 5** for participant 2). The observations from these results are discussed below.

1. There were significant differences when velocity was over 80 km/h, especially when velocity was 90–110 km/h or more for participant 1.
2. Participant 2 experienced obvious changes in subjective risk at velocities of 50–60 km/h and 70–80 km/h.
3. These results not only confirm that subjective risk is correlated with velocity, but also confirm the variation in risk between individuals. Participants 1 and 2 exhibited different thresholds regarding their similar ranked sensitivity to velocity.

These results can be used in the future in the design of autonomous driving systems to make the experience more comfortable for passengers by incorporating their personalized velocity preferences.

5.1.2. Surrounding Vehicle Location Ranking

In a manner similar to our analysis of ego vehicle driving signals, we also conducted an experiment to determine the importance of various surrounding vehicle locations. The results of our feature importance analysis for surrounding vehicle TTCs are shown in **Fig. 14(a)** for lane changes to the left, and **Fig. 14(b)** for lane changes to the right. Before and during lane changes to the left, areas 1 and 2 showed significant importance. However after the lane changes, area 3 became more important, while area 2 became less important. Before and during lane changes to the right, areas 4 and 5 showed significant importance. However, after the lane changes areas 1–5 showed little difference in importance in relation to the subjective risk assessments of our participants. Obvious differences between our participants in the importance of the locations of surrounding vehicles during lane change scenes were hardly ever observed.

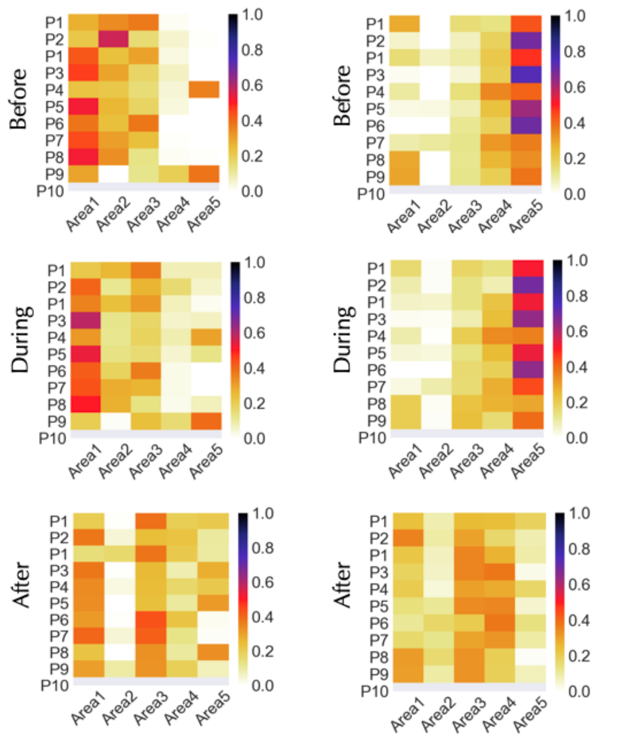

(a) Left lane changes (b) Right lane changes

Fig. 14. Analysis results for the feature importance of surrounding vehicle area for (a) left lane changes and (b) right lane changes. Obvious differences in the surrounding vehicle directions between individuals were rarely observed.

5.2. Prediction During Lane Changes

First, we conducted a participant-closed prediction using lane change data. The same participant's data was used in both training and test phases, the results of which represented the performance of our models under the condition where a large amount of participant-specific data could be prepared in advance. In order to evaluate several different models fairly, the test data selected to evaluate the first model was also used to evaluate the other models.

The purpose of this study was to apply data-driven approaches to predict the subjective risk perception levels of participants from measurable driving behavior signals, and surrounding vehicle information, rather than from demographic information. In addition, we propose BLSTM as our prediction method by comparing it with the following machine learning methods selected as benchmarks for their high performance in previous risk assessment or related tasks [10, 33, 50–54]:

1. AdaBoost (AB)
2. Random forests (RF)
3. Support vector machine (SVM)
4. Guassian process (GP)
5. Gaussian mixture models (GMM)
6. Multi-layer perceptron (MLP)
7. Long short-term memory (LSTM)
8. Bidirectional long short-term memory (BLSTM)

Table 3. Comparison of participant-closed risk prediction averaged AUC results for conventional and proposed methods, using ego vehicle risk features, surrounding vehicle risk features or an integration of ego and surrounding vehicle risk features.

	Ego vehicle	Surrounding vehicle	Integrate both
AB	0.648	0.535	0.642
SVM	0.612	0.540	0.623
GP	0.564	0.512	0.583
GMM	0.631	0.579	0.637
MLP	0.598	0.528	0.614
RF	0.641	0.606	0.680
LSTM	0.653	0.626	0.692
BLSTM	**0.670**	**0.636**	**0.703**

To compare under the same conditions, *full models* were selected for subjective risk prediction using only during lane change data. A grid search procedure was implemented using a reduced dataset to find the optimal set of parameters for the conventional models. The detailed full model architecture using BLSTM is illustrated in **Fig. 9**. The results of this comparison experiment are shown in **Table 3**, which indicate that the BLSTM is the most appropriate method for assessing subjective risk. These results confirmed the BLSTM could be applied for capturing risk perception levels from sequential lane change maneuver data.

5.3. Forecasting Before Lane Changes

We conducted participant-closed and participant-open forecasting using 3 s of data before the start of lane change. In participant-open experiment, the data for different participants was used in the training and test phases. This experiment evaluated performance when participant-specific data could not be prepared in advance, and is an important indicator of viability for practical use. The experiment was conducted using leave-one-participant-out validation, where one participant's data were used as the test data, and the remaining data of the other participants were used as the training data. The experimental results are shown in **Fig. 15**.

From these results we can see that performance in the participant-open subjective risk forecasting was lower than in the participant-closed experiment for all participants. There are two reasons for the poorer risk forecasting performance in the participant-open experiment. Firstly, the perception of risk is participant-dependent (i.e., subjective) and thus it varies from person to person. It may vary so much that no single model can accurately reproduce the risk assessments of different drivers. Secondly, the factors that cause drivers to subjectively per-

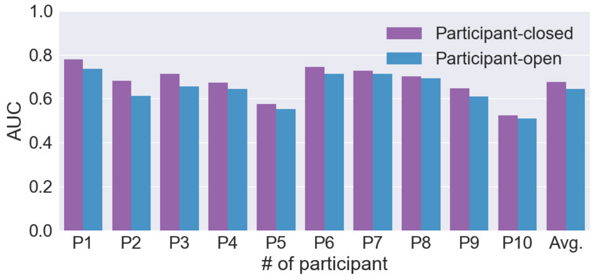

Fig. 15. Comparison of personalized subjective risk forecasting accuracy for participant-closed and participant-open experiment.

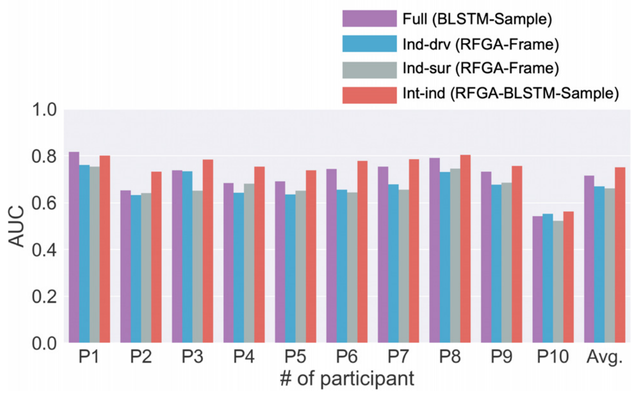

Fig. 16. Comparison of personalized subjective risk prediction accuracy using full model (BLSTM-sample), individual model based on ego vehicle driving signals (ind-drv-RFGA-frame), individual model based on surrounding vehicle information (ind-sur-RFGA-frame), and integrated individual model (int-ind-RFGA-BLSTM-sample).

ceive the presence of risk not only depend on the ego vehicle driving signals and the locations of surrounding vehicles, but also may be caused by other factors, such as phenomena in the surrounding environment, and the personality or emotional state of the driver.

5.4. Subjective Risk Assessment Result

Finally, as mentioned in Section 4.4, we proposed three types of framework for subjective risk prediction: a full model, an individual model and an integrated individual model. In order to validate our proposed models, we built four models for comparison that are defined below.

1. Full (BLSTM-sample) model: lane change maneuver data, including ego vehicle driving signals and surrounding vehicle information for the full length of time, were regarded as one sample, and each sample corresponded to one risk label.

2. Individual model based on ego vehicle driving signal (ind-drv-RFGA-frame): lane change maneuver data included only ego vehicle driving signals, and each frame corresponded to one risk label.

3. Individual model based on surrounding vehicle information (ind-sur-RFGA-frame): lane change maneuver data include surrounding vehicle information, and each frame corresponded to one risk label.

4. Integrated individual model (int-ind-RFGA-BLSTM-sample): lane change maneuver data, including ego vehicle driving signals and surrounding vehicle information with whole time length are regarded as one sample, and each sample corresponded to one risk label. Logistic regressions are conducted to combine two prediction results to decide the weight of individual differences and sequential information.

Our research goals were firstly to understand the individual differences on driving signals related to risk perception, and to improve risk prediction accuracy for different participants. Our integrated individual model satisfied these two goals within one model. The experimental results from the comparison of model variations are shown in **Fig. 16**. The proposed PSDRM with integrated individual structure showed the best subjective risk prediction performance for all participants significantly. This result showed that by combining RFGA and BLSTM, the PSDRM could capture individual differences of risk factors, and at the same time, it could predict subjective risk levels properly.

6. Discussion

We proposed an RF based explainable approach to identify personalized factors extracted from subjective assessment of driving risk. Data-driven approaches can give us insights into human perception which cannot easily to be described directly. Moreover, this approach can provide a quantifiable way to utilize and optimize driving behavior to reduce risk perception for specific drivers or passengers. The comparison results between participant-closed and participant-open experiments, showed that for all participants, the participant-closed which only use the data of specific participant for subjective risk modeling obtained slightly better accuracy than the participant-open models. This result confirmed that subjective risk perception is influenced by an individuals' personal factors, and by using those factors, the proposed integrated individual model achieved better risk assessment performance. However, we still face the difficulties because of lack of sufficient data to model individual differences and to predict subjective risk accurately. For example, for participants 2 and 5, and especially participant 10, we could not improve his/her prediction accuracy to an acceptable level with any of the models. This limitation included investigation of individual differences in subjective risk perception. Data were collected from only ten participants. The small number of participants may have resulted in some of the key factors that influence risk perception being randomized with noise. Another limitation of this study was that the participants were only able to obtain lane change information from forward-facing video camera footage without experiencing acceleration directly. The result of our experiment to validate the lane change segments indicated that participants perceived the period during lane changes to be the riskiest, compared with the time periods before and after the lane change. However, because the participants based their risk assessment feedback on videos of the road ahead, this could also indicate that our experiment omitted important information needed for risk assessment that was not included in the video footage.

The field of subjective risk assessment and subjective risk factor analysis is still in its infancy. The real-time driving data recording systems and cloud platform services that have emerged in recent years have facilitated the collection and analysis of data for real-world driving behavior, and further data-driven research using these new technologies will help to better understand how drivers assess risk. We aimed to draw a light from the rapidly increasing data-driven methods into risk perception modeling and utilize this knowledge to improve personalized autonomous driving in future.

7. Conclusion and Future Work

In this study, we attempted to model subjective risk by analyzing individual differences in the importance of ego vehicle driving signals and surrounding vehicle locations when the study participants predicted the risk levels of expressway lane changes. We proposed a PSDRM for modeling subjective perception of risk. Our proposed model is an integrated framework consisting of an RFGA risk factor identifier, which is based on an RF optimized using GAs, to extract the personalized parameters needed to model subjective risk. A BLSTM subjective risk predictor was then employed to estimate the potential risk level of lane change maneuvers as perceived by different individuals (our study participants). Experiments using our data-driven risk factor identifier intuitively confirm the existence of individual differences in the subjective risk perception for individuals viewing the same lane change videos. The features that influenced risk perception during driving were extracted using driving related factors from two categories: ego vehicle driving signals and surrounding vehicle locations. Data within these two categories could be directly measured and extracted in real-time, unlike other predictive factors such as the personality or demographic information collected using questionnaires. Another contribution of this study was the discovery that by capturing individual differences in influential risk factors along with time series data, the subjective risk level prediction accuracy was increased for several of the participants. In the future, we will expand on this work to capture personalized preferences using driving-related signals, and develop methods to adjust the behavior of automated vehicles by building a human-in-the-loop personalized driving system that can adapt to user preferences.

Acknowledgements

The authors would like to thank the Japanese New Energy and Industrial Technology Development Organizations strategic program on Artificial Intelligence (NEDO-AI) for their inspiration and support.

References:

[1] Y. Zhang, E. K. Antonsson, and K. Grote, "A new threat assessment measure for collision avoidance systems," Proc. of 2006 IEEE Intelligent Transportation Systems Conf., pp. 968-975, 2006.

[2] C. Laugier, I. E. Paromtchik, M. Perrollaz, M. Yong, J.-D. Yoder, C. Tay, K. Mekhnacha, and A. Nègre, "Probabilistic analysis of dynamic scenes and collision risks assessment to improve driving safety," IEEE Intelligent Transportation Systems Magazine, Vol.3, No.4, pp. 4-19, 2011.

[3] Y. Zheng, J. Wang, X. Li, C. Yu, K. Kodaka, and K. Li, "Driving risk assessment using cluster analysis based on naturalistic driving data," Proc. of 17th Int. IEEE Conf. on Intelligent Transportation Systems (ITSC), pp. 2584-2589, 2014.

[4] S. Lefèvre, D. Vasquez, and C. Laugier, "A survey on motion prediction and risk assessment for intelligent vehicles," Robomech J., Vol.1, 1, 2014.

[5] X. Wang, M. Chen, M. Zhu, and P. Tremont, "Development of a kinematic-based forward collision warning algorithm using an advanced driving simulator," IEEE Trans. on Intelligent Transportation Systems, Vol.17, No.9, pp. 2583-2591, 2016.

[6] U. Tränkle, C. Gelau, and T. Metker, "Risk perception and age-specific accidents of young drivers," Accident Analysis and Prevention, Vol.22, No.2, pp. 119-125, 1990.

[7] G. B. Grayson, G. Maycock, J. A. Groeger, S. M. Hammond, and D. T. Field, "Risk, hazard perception and perceived control," TRL Report TRL560, TRL Ltd., Crowthorne, UK, 2003.

[8] M. Horswill and F. Mckenna, "Drivers' hazard perception ability: Situation awareness on the road," S. Banbury and S. Tremblay (Eds.), "A cognitive approach to situation awareness: Theory and application," pp. 155-175, Routledge, 2004.

[9] D. Fisher and D. Strayer, "Modeling situation awareness and crash risk," Annals of Advances in Automotive Medicine / Annual Scientific Conf., Association for the Advancement of Automotive Medicine. Association for the Advancement of Automotive Medicine. Scientific Conf., Vol.58, pp. 33-39, 2014.

[10] P. Ping, Y. Sheng, W. Qin, C. Miyajima, and K. Takeda, "Modeling driver risk perception on city roads using deep learning," IEEE Access, Vol.6, pp. 68850-68866, 2018.

[11] M. Edmonds, F. Gao, H. Liu, X. Xie, S. Qi, B. Rothrock, Y. Zhu, Y. N. Wu, H. Lu, and S.-C. Zhu, "A tale of two explanations: Enhancing human trust by explaining robot behavior," Science Robotics, Vol.4, No.37, eaay4663, 2019.

[12] T. Kondoh, T. Hirose, and N. Fuyuyama, "A proposal of tailor-made risk feeling formula when closing on the lead vehicle," The Japanese J. of Ergonomics, Vol.50, pp. 350-358, 2014.

[13] S. McGill, G. Rosman, T. Ort, A. Pierson, I. Gilitschenski, B. Araki, L. Fletcher, S. Karaman, D. Rus, and J. Leonard, "Probabilistic risk metrics for navigating occluded intersections," IEEE Robotics and Automation Letters, p. 1, 2019.

[14] D. Sato, E. Nunobiki, S. Inoue, and P. Raksincharoensak, "Motion planning and control in highway merging maneuver based on dynamic risk potential optimization," Proc. of 5th Int. Symp. on Future Active Safety Technology Towards Zero-Traffic-Accidents (FAST-zero'19), pp. 1-6, 2019.

[15] S. Kitajima, Y. Marumo, T. Hiraoka, and M. Itoh, "Comparison of evaluation indices concerning estimation of driver's risk perception," Review of Automotive Engineering, Vol.30, No.2, pp. 191-198, 2009.

[16] B. Wu, X. Zhu, J. Shen, and L. Li, "A study on risk assessment algorithm based on natural driving data," Automotive Engineering, Vol.39, No.8, pp. 907-914, 2017.

[17] H. Mao, X. Deng, D. Lord, G. Flintsch, and F. Guo, "Adjusting finite sample bias in traffic safety modeling," Accident Analysis and Prevention, Vol.131, pp. 112-121, 2019.

[18] Y. Fujinami, P. Raksincharoensak, D. Ulbricht, and R. Adomat, "Risk predictive driver assistance system for collision avoidance in intersection right turns," J. Robot. Mechatron., Vol.30, No.1, pp. 15-23, 2018.

[19] R. Fuller, "Towards a general theory of driver behaviour," Accident Analysis and Prevention, Vol.37, No.3, pp. 461-472, 2005.

[20] G. J. S. Wilde, "Target Risk 2: A New Psychology of Safety and Health – What Works? What Doesn't? And Why...," Pde Pubns, 2001.

[21] S. G. Charlton, N. J. Starkey, J. A. Perrone, and R. B. Isler, "What's the risk? A comparison of actual and perceived driving risk," Transportation Research Part F: Traffic Psychology and Behaviour, Vol.25, pp. 50-64, 2014.

[22] H. Huang, Y. Li, X. Zheng, J. Wang, Q. Xu, and S. Zheng, "Objective and subjective analysis to quantify influence factors of driving risk," Proc. of 2019 IEEE Intelligent Transportation Systems Conf. (ITSC), pp. 4310-4316, 2019.

[23] P. Ulleberg and T. Rundmo, "Personality, attitudes and risk perception as predictors of risky driving behaviour among young drivers," Safety Science, Vol.41, No.5, pp. 427-443, 2003.

[24] F. W. Siebert, M. Oehl, and H.-R. Pfister, "The influence of time headway on subjective driver states in adaptive cruise control," Transportation Research Part F: Traffic Psychology and Behaviour, Vol.25, pp. 65-73, 2014.

[25] F. W. Siebert, M. Oehl, F. Bersch, and H.-R. Pfister, "The exact determination of subjective risk and comfort thresholds in car following," Transportation Research Part F: Traffic Psychology and Behaviour, Vol.46, Part A, pp. 1-13, 2017.

[26] H. Aoki, N. V. Q. Hung, and H. Yasuda, "Perceptual risk estimate (pre): an index of the longitudinal risk estimate," Proc. of 22nd Enhanced Safety of Vehicles Conf., 11-0121, 2011.

[27] T. Rundmo, "Associations between risk perception and safety," Safety Science, Vol.24, No.3, pp 197-209, 1996.

[28] X. Cai, C. Wang, S. Chen, and J. Lu, "Model development for risk assessment of driving on freeway under rainy weather conditions," PLOS ONE, Vol.11, e0149442, 2016.

[29] Y. Wang, L. Li, L. Feng, and H. Peng, "Professional Drivers' Views on Risky Driving Behaviors and Accident Liability: A Questionnaire Survey in Xining, China," Transportation Letters, Vol.6, No.3, pp. 126-135, 2014.

[30] S. Jafarpour and V. Rahimi-Movaghar, "Determinants of risky driving behavior: a narrative review," Medical J. of the Islamic Republic of Iran, Vol.28, p. 142, 2014.

[31] T. A. Dingus, F. Guo, S. Lee, J. F. Antin, M. Perez, M. Buchanan-King, and J. Hankey, "Driver crash risk factors and prevalence evaluation using naturalistic driving data," Proc. of the National Academy of Sciences, Vol.113, No.10, pp. 2636-2641, 2016.

[32] F. Guo and Y. Fang, "Individual driver risk assessment using naturalistic driving data," Accident Analysis and Prevention, Vol.61, pp. 3-9, 2013.

[33] N. Bao, C. Miyajima, E. Takeuchi, and K. Takeda, "Estimating risk levels perceived by individuals for lane change scenes," Proc. of the 4th Int. Symp. on Future Active Safety Technology Toward Zero Accidents (FAST-zero), pp. 1-6, 2017.

[34] L. Breiman, "Random forests," Machine Learning, Vol.45, No.1, pp. 5-32, 2001.

[35] B. Kim, D. M. Malioutov, and K. R. Varshney, "Proceedings of the 2016 ICML workshop on human interpretability in machine learning (WHI 2016)," arXiv:1607.02531, 2016.

[36] D. Gunning, "Darpa's explainable artificial intelligence (xai) program," IUI '19: Proc. of the 24th Int. Conf. on Intelligent User Interfaces, p. ii, 2019.

[37] G. Louppe, "Understanding random forests: From theory to practice," arXiv:1407.7502, 2014.

[38] R. Genuer, J.-M. Poggi, and C. Tuleau-Malot, "Variable selection using random forests," Pattern Recognition Letters, Vol.31, No.14, pp. 2225-2236, 2010.

[39] K. Takeda, J. H. L. Hansen, P. Boyraz, L. Malta, C. Miyajima, and H. Abut, "International large-scale vehicle corpora for research on driver behavior on the road," IEEE Trans. on Intelligent Transportation Systems, Vol.12, No.4, pp. 1609-1623, 2011.

[40] E. Allen and C. A. Seaman, "Likert scales and data analyses," Quality Progress, pp. 64-65, 2007.

[41] C. Miyajima, Y. Nishiwaki, K. Ozawa, T. Wakita, K. Itou, K. Takeda, and F. Itakura, "Driver modeling based on driving behavior and its evaluation in driver identification," Proc. of the IEEE, Vol.95, No.2, pp. 427-437, 2007.

[42] L. J. P. van der Maaten and G. E. Hinton, "Visualizing high-dimensional data using t-sne," J. of Machine Learning Research, Vol.9, pp. 2579-2605, 2008.

[43] P. G. Gipps, "A model for the structure of lane-changing decisions," Transportation Research Part B: Methodological, Vol.20, No.5, pp. 403-414, 1986.

[44] A. T. Azar, H. I. Elshazly, A. E. Hassanien, and A. M. Elkorany, "A random forest classifier for lymph diseases," Computer Methods and Programs in Biomedicine, Vol.113, No.2, pp. 465-473, 2014.

[45] E. Elyan and M. M. Gaber, "A genetic algorithm approach to optimising random forests applied to class engineered data," Information Sciences, Vol.384, pp. 220-234, 2017.

[46] M. Schuster and K. Paliwal, "Bidirectional recurrent neural networks," IEEE Trans. on Signal Processing, Vol.45, pp. 2673-2681, 1997.

[47] F. Weninger, J. Bergmann, and B. Schuller, "Introducing CURRENNT: The Munich Open-Source CUDA RecurREnt Neural Network Toolkit," The J. of Machine Learning Research, Vol.16, No.1, pp. 547-551, 2015.

[48] F. A. Gers, J. Schmidhuber, and F. Cummins, "Learning to forget: Continual prediction with lstm," IET, 1999.

[49] F. Zhang, C. Hu, Q. Yin, W. Li, H. Li, and W. Hong, "Multi-Aspect-Aware Bidirectional LSTM Networks for Synthetic Aperture Radar Target Recognition," IEEE Access, Vol.5, pp. 26880-26891, doi: 10.1109/ACCESS.2017.2773363, 2017.

[50] S. Lefévre, A. Carvalho, and F. Borrelli, "A learning-based framework for velocity control in autonomous driving," IEEE Trans. on Automation Science and Engineering, Vol.13, No.1, pp. 32-42, 2016.

[51] C. Vallon, Z. Ercan, A. Carvalho, and F. Borrelli, "A machine learning approach for personalized autonomous lane change initiation and control," 2017 IEEE Intelligent Vehicles Symp. (IV), pp. 1590-1595, 2017.

[52] S. Ramyar, A. Homaifar, S. Salaken, S. Nahavandi, and A. Kurt, "A personalized highway driving assistance system," 2017 IEEE Intelligent Vehicles Symp. (IV), pp. 1596-1601, 2017.

[53] N. Bao, D. Yang, A. Carballo, Ü. Özgüner, and K. Takeda, "Personalized safety-focused control by minimizing subjective risk," Proc. of 2019 IEEE Intelligent Transportation Systems Conf. (ITSC), pp. 3853-3858, 2019.

[54] C. E. Rasmussen, "Gaussian processes in machine learning," O. Bousquet, U. von Luxburg, G. Rätsch (Eds), "Advanced Lectures on Machine Learning," pp. 63-71, Springer, 2004.

Appendix A. One-Way ANOVA Between Velocity and Subjective Risk Perception

The test scores of one-way ANOVA between velocity and subjective risk perception for participants 1 and 2 are shown in **Tables 4** and **5**, respectively.

Table 4. One-way ANOVA between velocity and subjective risk perception for participant 1.

Velocity [km/h]	Difference	lwr	upr	p
20–30	0.112	0.004	0.240	0.0037
30–40	0.264	0.146	0.382	0.001
40–50	0.463	0.345	0.581	0.001
50–60	0.402	0.284	0.520	0.001
60–70	0.364	0.245	0.4820	0.001
70–80	0.280	0.162	0.398	0.001
80–90	0.138	0.020	0.256	0.009
90–100	0.017	−0.101	0.247	0.020
100–110	−0.061	−0.179	0.057	0.804

Table 5. One-way ANOVA between velocity and subjective risk perception for participant 2.

Velocity [km/h]	Difference	lwr	upr	p
20–30	−0.148	−0.349	0.052	0.346
30–40	−0.697	−0.898	−0.496	0.001
40–50	−0.863	−1.064	0.581	0.001
50–60	−0.094	−0.295	0.107	0.879
60–70	−0.217	−0.418	−0.016	0.023
70–80	0.055	−0.146	0.256	0.995
80–90	0.271	0.071	0.472	0.0001
90–100	0.666	0.465	0.867	0.000
100–110	−0.166	−0.367	0.035	0.202

Name:
Naren Bao

Affiliation:
Graduate School of Informatics, Nagoya University

Address:
Furo-cho, Chikusa-ku, Nagoya 464-8601, Japan

Brief Biographical History:
2008 Received B.E. in Software Engineering from Tianjin University
2008-2014 Software Engineer, COMNET Inc. / T.M.C.
2015- Assistant, Graduate School of Informatics, Nagoya University
2018 Received M.E. in Information Science from Nagoya University

Main Works:
• "Personalized Safety-focused Control by Minimizing Subjective Risk," Proc. of 2019 IEEE Intelligent Transportation Systems Conf. (ITSC), pp. 3853-3858, 2019.

Membership in Academic Societies:
• The Institute of Electrical and Electronics Engineers (IEEE)

Name:
Alexander Carballo

Affiliation:
Designated Assistant Professor, Institutes of Innovation for Future Society, Nagoya University

Address:
Furo-cho, Chikusa-ku, Nagoya 464-8601, Japan

Brief Biographical History:
2011 Received Ph.D. from Intelligent Robot Laboratory, Tsukuba University
2011-2017 Research and Development, Hokuyo Automatic Co., Ltd.
2016- Part-time Lecturer, Graduate School of Engineering, Osaka City University
2017- Designated Assistant Professor, Nagoya University

Main Works:
• "End-to-End Autonomous Mobile Robot Navigation with Model-Based System Support," J. Robot. Mechatron., Vol.30, No.4, pp. 563-583, 2018 (received JRM Best Paper Award 2019).
• "High Density Ground Maps using Low Boundary Height Estimation for Autonomous Vehicles," IEEE Int. Conf. on Intelligent Transportation Systems (ITSC), pp. 3811-3818, 2018.
• "Training Engineers in Autonomous Driving Technologies using Autoware," IEEE Int. Conf. on Intelligent Transportation Systems (ITSC), pp. 3347-3354, 2019.
• "LIBRE: The Multiple 3D LiDAR Dataset," accepted for presentation at IEEE Intelligent Vehicles Symp. (IV), 2020.

Membership in Academic Societies:
• The Institute of Electrical and Electronics Engineers (IEEE)
• The Robotics Society of Japan (RSJ)
• The Asia-Pacific Signal and Information Processing Association (APSIPA)

Name:
Chiyomi Miyajima

Affiliation:
Associate Professor, Daido University

Address:
10-3 Takiharu-cho, Minami-ku, Nagoya 457-8530, Japan

Brief Biographical History:
1996/1998/2001 Received B.E., M.E., and Ph.D. in Computer Science from Nagoya Institute of Technology
2001-2003 Research Associate, Department of Computer Science, Nagoya Institute of Technology
2003-2016 Assistant Professor, Graduate School of Information Science, Nagoya University
2016-2018 Designated Associate Professor, Institutes of Innovation for Future Society, Nagoya University
2018- Associate Professor, Daido University

Main Works:
- Analysis and the modeling of driver behavior
- Received Best Paper Awards at ICVES'09, FAST-zero'13, and ITSC'16

Membership in Academic Societies:
- The Institute of Electrical and Electronics Engineers (IEEE)
- Society of Automotive Engineers of Japan (JSAE)
- The Institute of Electronics, Information and Communication Engineers (IEICE)
- Acoustical Society of Japan (ASJ)

Name:
Eijiro Takeuchi

Affiliation:
Associate Professor, Graduate School of Informatics, Nagoya University

Address:
Furo-cho, Chikusa-ku, Nagoya 464-8601, Japan

Brief Biographical History:
2008-2014 Assistant Professor, Tohoku University
2014-2016 Designated Associate Professor, Nagoya University
2016- Associate Professor, Nagoya University

Main Works:
- "A 3-D Scan Matching using Improved 3-D Normal Distributions Transform for Mobile Robotic Mapping," IEEE/RSJ Int. Conf. on Intelligent Robots and Systems (IROS), pp. 3068-3073, 2006.

Membership in Academic Societies:
- The Japan Society of Mechanical Engineering (JSME)
- The Robotics Society of Japan (RSJ)
- The Society of Instrument and Control Engineers (SICE)
- The Institute of Electrical and Electronics Engineers (IEEE)

Name:
Kazuya Takeda

Affiliation:
Professor, Institutes of Innovation for Future Society / Graduate School of Informatics, Nagoya University

Address:
Furo-cho, Chikusa-ku, Nagoya 464-8601, Japan

Brief Biographical History:
1983/1985 Received B.E./M.E. degrees in Electrical Engineering from Nagoya University
1986-1989 Advanced Telecommunication Research Laboratories (ATR)
1987-1988 Visiting Scientist, Massachusetts Institute of Technology
1989-1995 Researcher and Research Supervisor, KDD Research and Development Laboratories
1994 Received Doctor of Engineering degree from Nagoya University
1995-2003 Associate Professor, Faculty of Engineering, Nagoya University
2003- Professor, Department of Media Science, Graduate School of Information Science, Nagoya University

Main Works:
- Media signal processing and its applications, including spatial audio, robust speech recognition and driving behavior modeling

Membership in Academic Societies:
- The Institute of Electrical and Electronics Engineers (IEEE) Intelligent Transportation Systems Society (ITSS), Member of the Board of Governors
- The Asia-Pacific Signal and Information Processing Association (APSIPA), Member of the Board of Governors